



Estimating heavy metals absorption efficiency in an aqueous solution using nanotube-type halloysite from weathered pegmatites and a novel Harris hawks optimization-based multiple layers perceptron neural network

Bui Hoang Bac^{1,2} · Hoang Nguyen^{3,4} · Nguyen Thi Thanh Thao¹ · Vo Thi Hanh^{2,5} · Le Thi Duyen^{2,5} · Nguyen Tien Dung¹ · Nguyen Khac Du¹ · Nguyen Huu Hiep^{2,6}

Received: 24 February 2021 / Accepted: 18 June 2021

© The Author(s), under exclusive licence to Springer-Verlag London Ltd., part of Springer Nature 2021

Abstract

In this study, nanotube-type halloysites from weathered pegmatites were investigated to absorb Pb^{2+} in an aqueous solution. Also, a novel hybrid intelligent model based on the multiple layers perceptron (MLP) neural network and the Harris hawks optimization (HHO) algorithm (i.e., HHO-MLP neural network) was proposed for estimating the absorption of Pb^{2+} from an aqueous solution using this novel material. XRD, SEM–EDS, and TEM analysis revealed the existence of overlapping tubular halloysites in the studied sample, similar to the results of previous studies. Various conditions of contact time, solution pH, the adsorbent weight, and Pb^{2+} initial concentration were considered and evaluated using batch adsorption experiments with a total of 53 cases. Subsequently, an HHO-MLP neural network was developed and applied to predict Pb^{2+} absorption efficiency in water by the nanotube-type halloysite from weathered pegmatites. A traditional MLP neural network model (without optimized by the HHO algorithm) was also investigated to predict and compare with that of the proposed HHO-MLP neural network model. The experimental results indicated that the nanotube-type halloysite from weathered pegmatites is a potential material used in processing water and removing heavy metals, i.e., Pb^{2+} , with a promising development. Furthermore, the obtained results of the proposed HHO-MLP neural network model showed that this model is a robust intelligent model for estimating the efficiency of the Pb^{2+} absorption in water using nanotube-type halloysite from weathered pegmatites (i.e., MSE = 1.647; RMSE = 1.283; $R^2 = 0.931$). It can be applied to increase the Pb^{2+} absorption efficiency to eliminate Pb^{2+} in an aqueous solution.

Keywords Water · Nanotube-type halloysite · Heavy metals · Absorption · Artificial intelligence · Weathered pegmatites

✉ Bui Hoang Bac
buihoangbac@humg.edu.vn

✉ Hoang Nguyen
nguyenhoang@humg.edu.vn

¹ Department of Exploration Geology, Faculty of Geosciences and Geoengineering, Hanoi University of Mining and Geology, 18 Vien St., Duc Thang Ward, Bac Tu Liem Dist., Hanoi, Vietnam

² Centre for Excellence in Analysis and Experiment, Hanoi University of Mining and Geology, 18 Vien St., Duc Thang Ward, Bac Tu Liem Dist., Hanoi, Vietnam

³ Department of Surface Mining, Mining Faculty, Hanoi University of Mining and Geology, 18 Vien St., Duc Thang Ward, Bac Tu Liem Dist., Hanoi 100000, Vietnam

⁴ Innovations for Sustainable and Responsible Mining (ISRMI) Group, Hanoi University of Mining and Geology, 18 Vien St., Duc Thang Ward, Bac Tu Liem Dist., Hanoi 100000, Vietnam

⁵ Department of Chemistry, Faculty of Basic Science, Hanoi University of Mining and Geology, 18 Vien St., Duc Thang Ward, Bac Tu Liem Dist., Hanoi, Vietnam

⁶ Department of Geology, Faculty of Geosciences and Geoengineering, Hanoi University of Mining and Geology, 18 Vien St., Duc Thang Ward, Bac Tu Liem Dist., Hanoi, Vietnam

1 Introduction

Over the last few decades, environmental contamination by heavy metals is considered the most dangerous effect among the numerous environmental pollutants, such as copper (Cu), cadmium (Cd), nickel (Ni), chromium (Cr), arsenic (As), thulium (Tl), mercury (Hg), dysprosium (Dy), lead (Pb), to name a few, are increased on a global scale due to rapid industrialization [1, 2]. They are considered the most adverse elements for human health and aquatic ecosystems [3–7]. In developing countries, these heavy metals are discharged to the environment from various industrial activities, such as mining, paints and batteries, smelting, tanning, to name a few. They persist in the soil and water environments for a very long time of their non-biodegradable nature [8, 9]. Then, they follow drinking water and the food chain to go to the human body.

Understanding the adverse effects of heavy metals, many researchers studied the absorption or removing heavy metals in water, wastewater, and soils. Of these environments, water is considered an essential objective because variance accounted for only 2.5% of the earth's freshwater [10, 11]. It is an indispensable requirement for the human body every day. To adsorb heavy metals from water, many biochar systems and materials have been proposed and applied. For instance, graphene oxide and its composites were studied and proposed as novel adsorbents to remove various heavy metals, i.e., Cd^{2+} , Cu^{2+} , and Ni^{2+} [12]. Many graphene oxide-based materials were also used to remove heavy metals in water [13]. In another study, Jiang et al. [14] proposed a novel bio-adsorbent for heavy metals' absorption, namely polyacrylamide oxide hydrogel grafted sodium alginate. Accordingly, Pb^{2+} and Cu^{2+} were removed, and more than 60% of absorption capacity was confirmed after five cycles. Another type of modified graphene oxide was also applied for eliminating Pb^{2+} and Cu^{2+} based on thiosemicarbazide nanocomposite [15]. Zhu et al. [16] evaluated and reviewed the feasibility, preparation, and mechanism of electrospun nanofibrous membranes (ELM) in removing heavy metals by using another material. Their review showed that ELM is a potential heavy metals-absorbing material in water. In another work, thiol-functionalized cellulose nanofiber membranes were also proposed by Choi et al. [17] for the absorption of Cu^{2+} , Cd^{2+} , and Pb^{2+} with a promising result. Also, many materials are used to adsorb heavy metals in water, and they can be referred to in literature [18–24].

Many researchers applied state-of-the-art techniques for estimating the heavy metals absorption performance of different materials by alternative approaches. Of those, artificial intelligence (AI) techniques are taken into account as potential solutions not only in water treatment, but also in

many other engineering problems [25–29]. In this regard, Singh et al. [30] applied the radial basis function (RBF) and multilayer perceptron (MLP) neural networks, support vector machine (SVM), and gene expression programming (GEP) to predict the adsorptive removal of chlorophenol (CP^{2+}). These models' outstanding performances were interpreted in their study, and MLPN and RBFN models were evaluated better than those of the other models. Fawzy et al. [31] also developed an ANN (artificial neural network) model for estimating the Cd^{2+} removal efficiency. A high fit was demonstrated in their study, with an R^2 of 0.923. Dolatabadi et al. [32] utilized an ANN and adaptive neuro-fuzzy inference system (ANFIS) model to predict heavy metals' removal process in aqueous using sawdust. Their results revealed that these models are promising simulation techniques for heavy metal removal processes from an aqueous solution. Besides, a critical review of different machine learning algorithms, such as ANN, genetic algorithm (GA), and particle swarm optimization (PSO), was employed by Fan et al. [33] in terms of removal processes modeling of heavy metals. Their conclusion indicated that the GA-ANN and PSO-ANN models could be successfully applied to model heavy metals' removal processes with satisfactory accuracy. By a similar method, Lu et al. [34] built ANN and SVM models to simulate the concentrations of heavy metals with a promising result. They claimed that the SVM and ANN models could simulate quickly particulate heavy metal concentrations. Given the improvement in the models' performance, Rahnama et al. [35] developed several RBFN and ANFIS-based models for predicting the sodium absorption rate of an aqueous solution, including ANFIS-GP (grid partitioning), ANFIS-SC (subtractive clustering), and ANFIS-FCM (fuzzy c-means clustering). Finally, the RBFN model was demonstrated as a proper model for sodium absorption prediction. Interesting work was also mentioned in the publication of El Hanandeh et al. [36] when they used ANN and multi-input multi-output (MIMO) models to predict the absorption capacity of heavy metals onto biochar with a promising result (i.e., $R^2 = 0.99$). The As^{2+} was also removed from water by Rodríguez-Romero et al. [37] using pyrolysis and ZnCl_2 activation. Subsequently, they modeled the absorption kinetics and isotherms results by an ANN model. Similar studies can be referred to in literature [38–46].

Based on the authors' best review, it can be seen that many materials and artificial intelligence techniques have been applied and proposed for heavy metals removal, as well as predicting the heavy metals absorption efficiency of various materials under different conditions. As an innovative approach in the present work, we investigated the feasibility of nanotube-type halloysite from weathered pegmatites in heavy metals' absorption. Herein, Pb^{2+} in an aqueous solution was selected as a case study since its

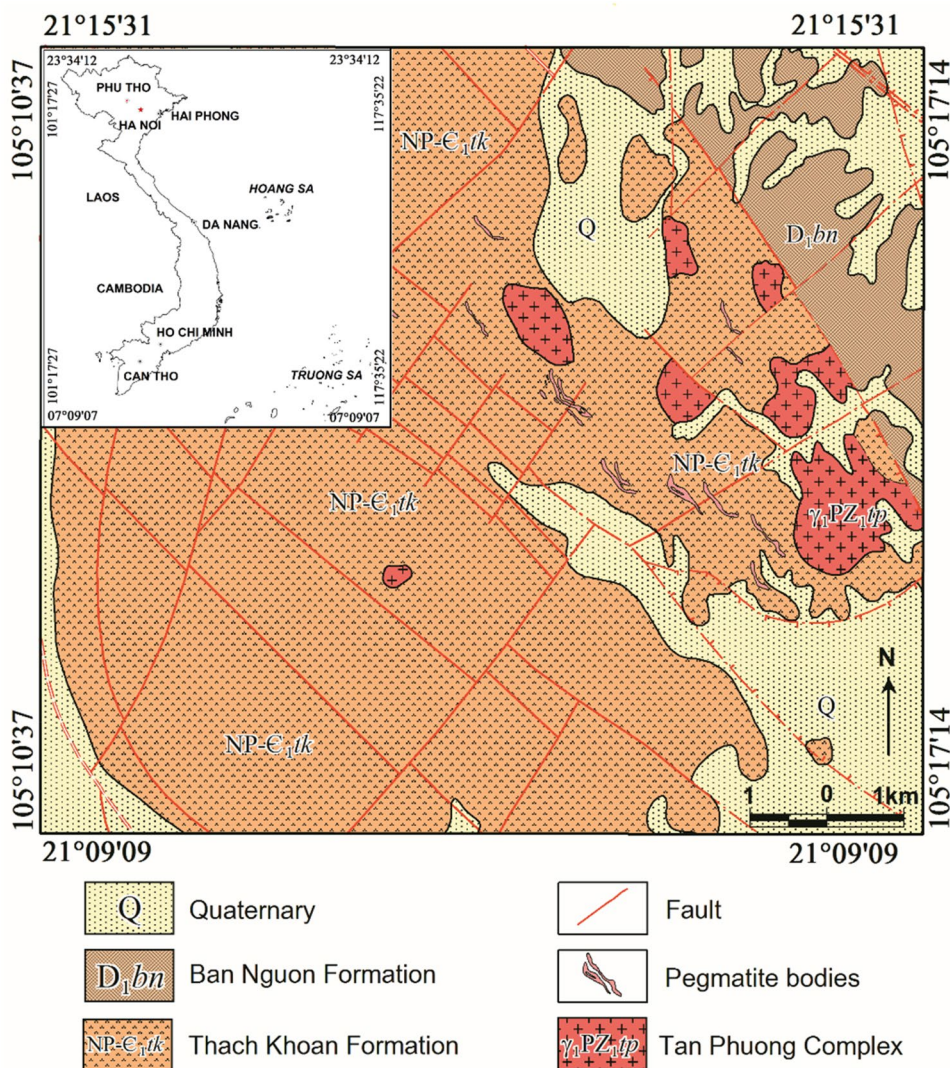
adverse health effects were warned by the World Health Organization (WHO) [47, 48], and nanotube-type halloysite weathered pegmatites was considered to remove Pb^{2+} in an aqueous solution. It is worth mentioning that nanotube-type halloysite from weathered pegmatites has not been investigated and used to absorb heavy metals. Next, a novel intelligent hybrid model was proposed to predict nanotube-type halloysite absorption efficiency from weathered pegmatites based on the MLP neural network and the Harris hawks optimization (HHO) algorithm, called HHO-MLP neural network model. It is worth noting that the HHO-MLP neural network model has not been developed to predict heavy metals' absorption in water. Finally, the Pb^{2+} absorption efficiency of the material (i.e., nanotube-type halloysite in weathered pegmatites) in an aqueous solution was thoroughly evaluated through experimental results, and the performance of the proposed

HHO-MLP neural network model in predicting the Pb^{2+} absorption efficiency was comprehensively assessed.

2 General geological setting of the Thach Khoan area

Thach Khoan area is located in Phu Tho province, about 85 km northwest of Hanoi's capital. The metamorphic Thach Khoan formation of the Proterozoic age (PR3-Є1tk) occupied most of the area, followed by sedimentary rocks of the early Devonian Ban Nguon Formation (D_1bn) and the Quaternary. Magma blocks related to the Late Paleozoic Tan Phuon granite complex scattered in the area. The major components of the igneous rocks are grey-white to grey-grey gillt granite, with banded structures. The mineral composition is mainly feldspar (45–75%), quartz (25–30%), and biotite (5–17%). There are many pegmatite bodies of

Fig. 1 Geological map of Thach Khoan area



the Tan Phuong complex in the area, with several hundred up to thousands of meters in length and tens to hundreds of meters wide. These bodies strike N60° to 80°W and have a dip of 50°–80° to the southwest (Fig. 1). The pegmatite bodies are weathered, and the weathering profile is up to 45–50 m. Tabular halloysites were identified in this weathered zone [49, 50].

3 Characterization of nanotube-type halloysite in weathered pegmatites

The sample was collected from the Lang Dong mineral processing plant in the Thach Khoan area, Phu Tho province, Vietnam. The sample was then well-mixed and separated to the particle size of < 32 μm by the wet sieving method. The separated sample (< 32 μm) was dried at 60 °C and used for subsequent analysis. Analytical methods used to determine the existence of tubular halloysites included X-ray diffraction analysis (XRD), scanning electron microscopy (SEM) with energy-dispersive X-ray spectroscopy (EDS), and transmission electron microscopy (TEM). The results are shown in Fig. 2.

XRD analysis result shows that the kaolin minerals are mainly minerals in the sample (Fig. 2A). Figure 2B presents the sample's SEM image with kaolin minerals in rod-shaped shapes overlapping to a matrix. The EDS result

for the mineral also indicates the presence of aluminum (Al), silicon (Si), and oxygen (O) elements, corresponding to the general chemical formula of the kaolin group ($\text{Al}_2\text{Si}_2\text{O}_5(\text{OH})_4 \cdot n\text{H}_2\text{O}$) (Fig. 2C). Significantly, the TEM analysis suggests that the rod-shaped kaolin minerals are halloysite minerals with distinct tubular structures (Fig. 2D). Thus, this study's results indicate that tubular halloysite minerals exist in the Thach Khoan sample, consistent with previous researches [49, 50].

4 Application of nanotube-type halloysite in removing Pb^{2+} and the experimental datasets

The experiments are conducted by adding a quantity of nanotubular halloysite powder to 50 mL of Pb^{2+} solution. The influence of different physicochemical parameters on the absorption process is examined. The initial concentrations of Pb^{2+} are prepared in the range of 20–80 mg/L. The contact time is varied from 10 to 120 min. The solutions' pH is adjusted in a range of about 3.00–6.8, and the dose of nanotubular halloysite powder changed from 0.3 to 0.9 g. The mixture is then shaken continuously at 100 rpm using a mechanical shaker at room temperature. After filtration to remove the solid, the remaining concentration of Pb^{2+} is determined by using inductively inducing plasma-mass

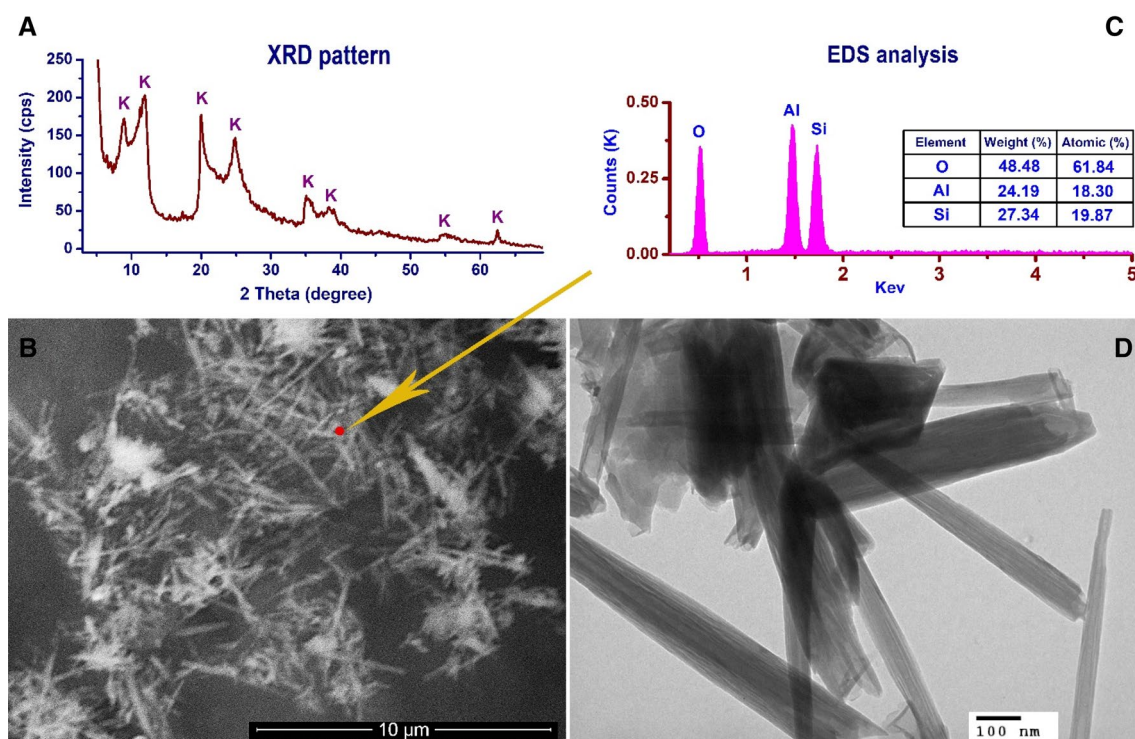


Fig. 2 XRD pattern (A), SEM image (B), EDS result (C), and TEM image (D) of the sample (O oxygen, Al aluminum, Si silicon, K kaolin).

spectrometric method (ICP-MS). Finally, a total of 53 experimental cases were performed, with each case comprising five factors of the initial concentration of Pb^{2+} ($Pb_{initial}$), solution pH (pH), the adsorbent weight (AW), contact time (CT), and the Pb^{2+} concentration after absorption (Pb_{output}). The results of the absorption are shown in Fig. 3, and the

details and characteristics of the dataset used are illustrated in Fig. 4.

From the visualization of the absorption dataset in Fig. 4, it can be seen that $Pb_{initial}$, pH, AW, and CT are potential input variables for predicting Pb_{output} since their correlation characteristics are very low. It should be fitted

Fig. 3 Pb^{2+} absorption efficiency using nanotube-type halloysite

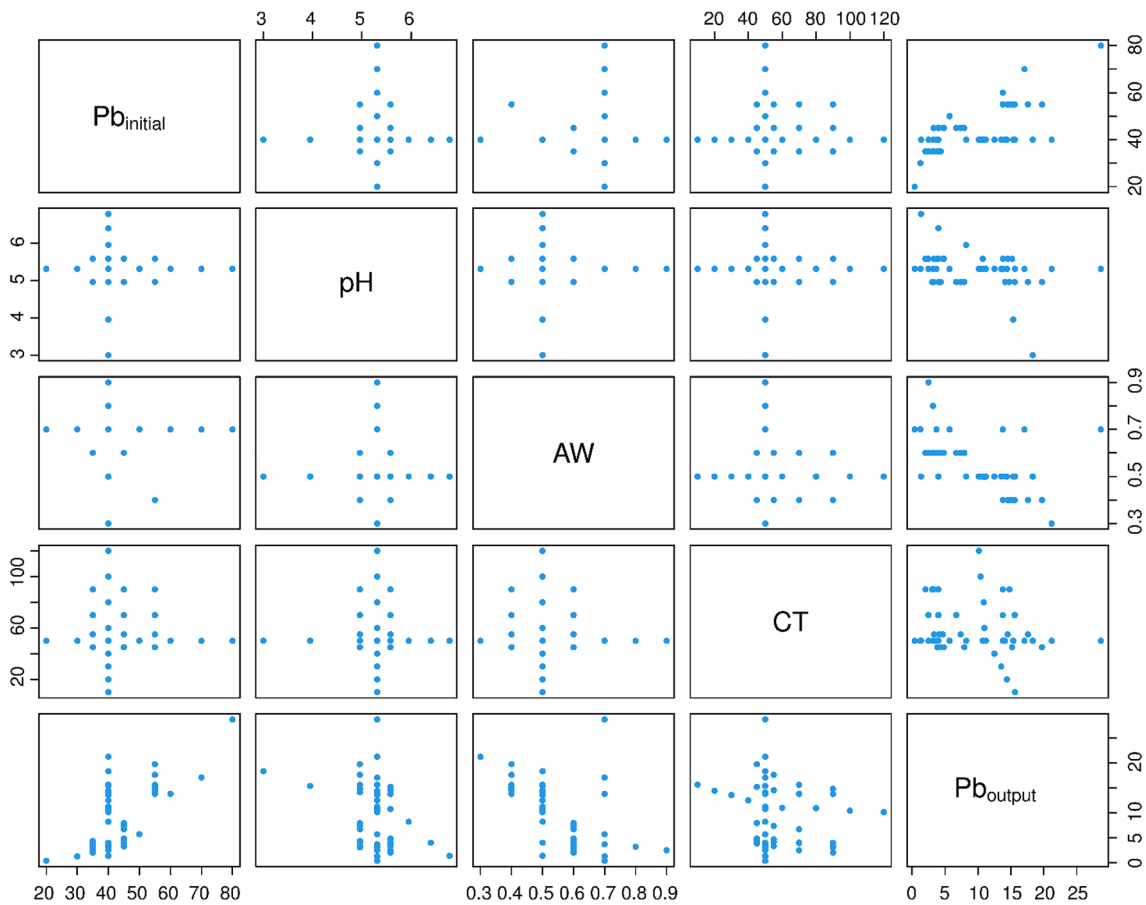
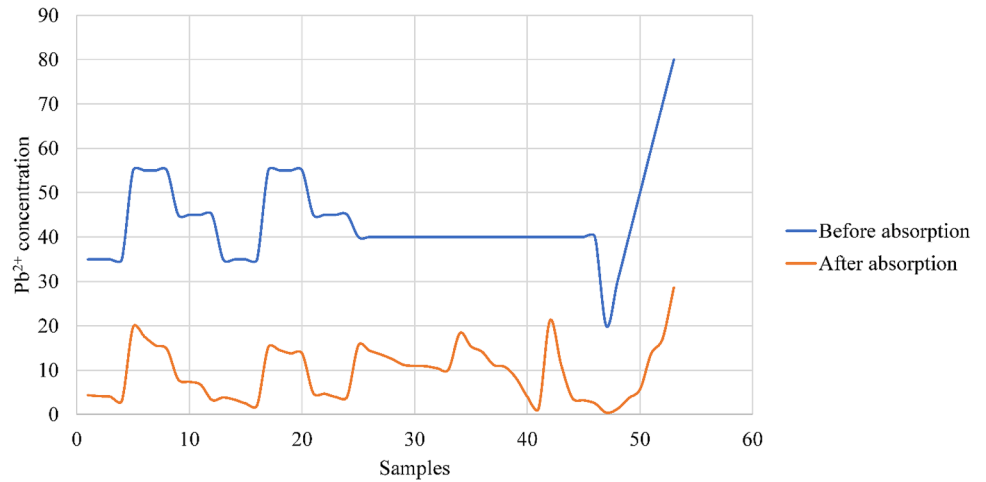


Fig. 4 Details of the characteristics and correlation of the absorption dataset

with a non-linear regression model, such as MLP neural network.

5 Background of MLP neural networks and HHO algorithm

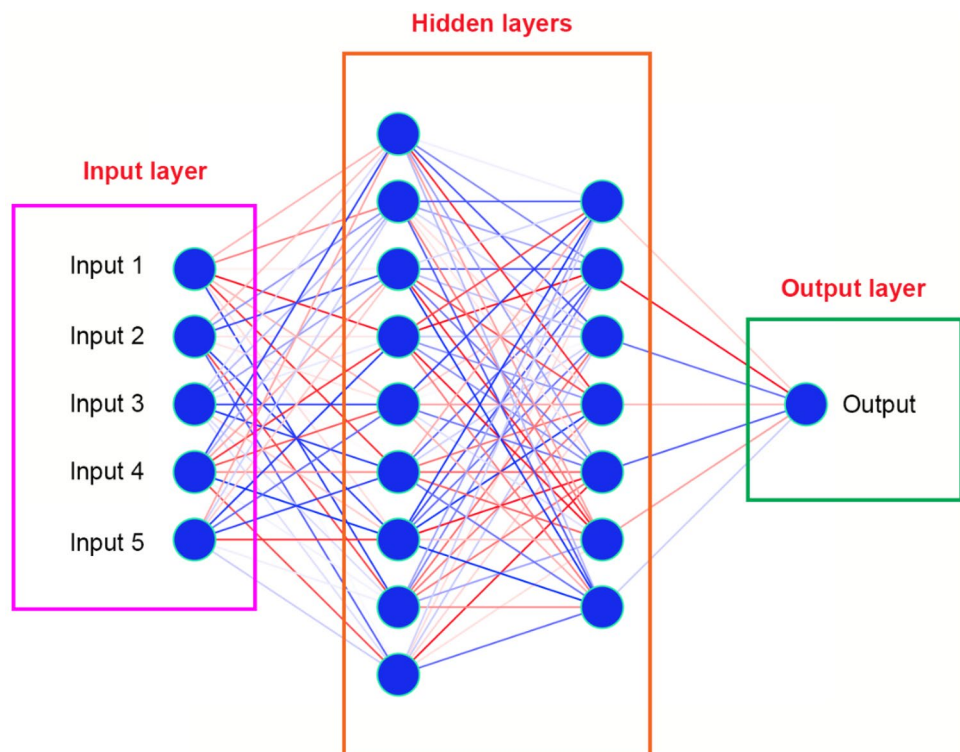
5.1 MLP neural networks

MLP neural networks are well known as a famous ANN structure, and it is a supervised learning algorithm aiming to train the ANN models [51, 52]. Like ANN, perceptrons are divided into many groups, and each group corresponds to a layer. At least three layers are included in an MLP neural network (i.e., input, hidden, and output layers) (Fig. 5). For more complicated MLP neural networks, two or more hidden layers are included. Hidden layers are taken into account as the dedicated computational engine of the MLP neural networks. MLP neural network's most advantages can effectively solve many nonlinear problems with promising results [53]. However, MLP neural network has some disadvantages with multiple hidden layers, such as a non-convex loss function with a local minimum, a requirement of tuning hidden layers, neurons, and iterations. Finally, it is sensitive to feature scaling [54]. It is a fact that an MLP neural network consists of one input layer, one or more hidden layers, and one output layer. The MLP neural networks with multiple hidden layers

are more complex, increasing the computational cost. In addition, complex MLP structures can face the overfitting problem. These disadvantages can lead to different validation accuracies or decrease MLP neural networks [55, 56]. In the MLP neural network, weights, biases, and activation functions are also crucial elements. Weights present the relationship between neurons (nodes), whereas biases are the threshold of the network. They are combined with increasing the performance of the model. Also, activation functions are often nonlinear functions used for expanding the prediction capable of neural networks. In other words, activation functions help the model learn about potentially complex nonlinear relationships in the data.

MLP neural networks were considered the foundation of deep learning during the past years, and they have been widely applied in many areas [57–62]. It has been successfully developed as a standalone model or optimized by many optimization algorithms to improve modeling accuracy. In this study, MLP neural network was selected to estimate and evaluate the Pb^{2+} absorption efficiency on nanotube-type halloysite in weathered pegmatites. The HHO algorithm was utilized to optimize the MLP, aiming to get an improvement of the MLP model in terms of the Pb^{2+} absorption efficiency estimation.

Fig. 5 Architecture of two-layer MLP neural network



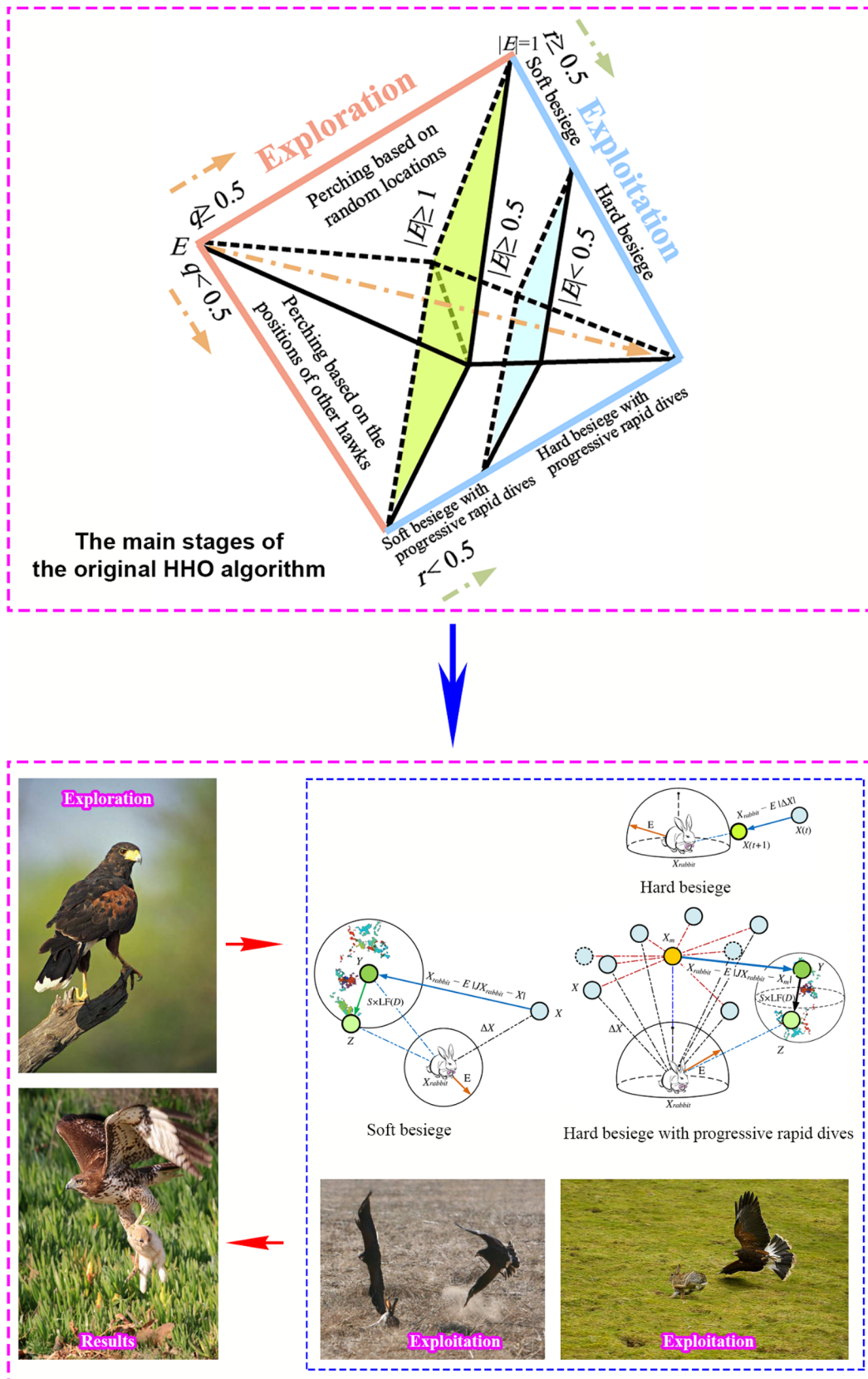


Fig. 6 Behaviors and strategies of Harris hawks for hunting the prey

5.2 HHO algorithm

HHO algorithm is a nature-based algorithm for optimization problems proposed by Heidari et al. [63]. It is inspired by the chasing style and cooperative behaviors of Harris hawks to surprise pounce a prey. These behaviors are divided into two phases: (1) exploration and (2) exploitation (Fig. 6).

In the first phase (i.e., exploration), Harris hawks perch on random positions to explore the prey using bright eyes as an outstanding advantage. Subsequently, they attack the prey surprise in the exploitation phase and apply several strategies to prevent the prey’s escape, such as soft besiege and hard besiege (Fig. 6). Further details and pseudo-code of the algorithm can be referred to in literature [52–66].

Inspired by the above behaviors of Harris hawks, Heidari et al. [63] developed and proposed the HHO algorithm for optimization problems, and it was quickly applied to many real-life problems with promising results [65, 67–74]. In this study, the HHO algorithm is applied to optimize the MLP neural network for estimating and evaluating the Pb²⁺ absorption efficiency on nanotube-type halloysite in weathered pegmatites, and the framework of this model is proposed in the next section.

6 Proposing the flowchart of the HHO-MLP neural network model

In the present work, a material, namely nanotube-type halloysite from weathered pegmatites, was investigated and selected to adsorb Pb²⁺ in an aqueous solution. Afterward, a novel intelligent hybrid model will be developed based on MLP neural network and HHO algorithm (i.e., HHO-MLP neural network) to evaluate and estimate the Pb²⁺ absorption efficiency of the material used. To this end, an MLP neural network will be developed at the first step with the initial weights. The HHO algorithm will then optimize this network through the optimization of the initial weights. To evaluate the obtained solutions of the HHO algorithm in optimizing the MLP neural network, mean-squared-error (MSE) is used as the fitness function, and the performance of the proposed HHO-MLP neural network model then will be verified through MSE values. The lowest value of MSE corresponds to the best HHO-MLP neural network model to estimate the Pb²⁺ absorption efficiency. The flowchart of the proposed HHO-MLP neural network is illustrated in Fig. 7.

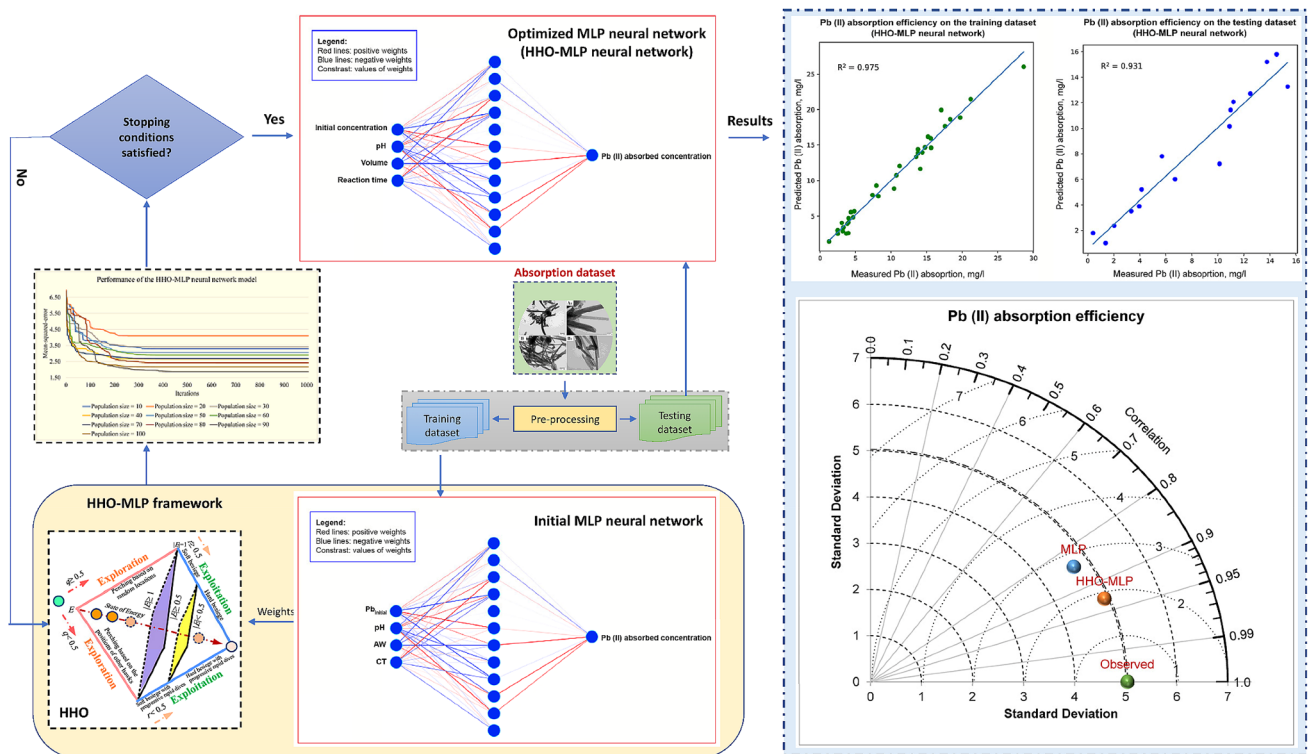


Fig. 7 Flowchart of the HHO-MLP neural network for estimating the Pb²⁺ absorption efficiency on nanotube-type halloysite

7 Development of the novel HHO-MLP neural network model

As described above, the primary objectives of this study are the material for Pb^{2+} absorption in an aqueous solution (i.e., nanotube-type halloysite in weathered pegmatites) and the development of the novel intelligent model HHO-MLP neural network for estimating the Pb^{2+} absorption efficiency of the material used. To this end, the proposed flowchart in Fig. 6 was applied.

Given the quality improvement of the MLP neural network model, architecture optimization of the MLP neural network model is necessary before developing the initial MLP neural network model for estimating the Pb^{2+} absorption efficiency on the nanotube-type halloysite in weathered pegmatites. The disadvantages of the MLP neural network were considered to prevent the reduction of the model's performance, as presented in Sect. 5.1. Also, the MinMax scaling method was applied to normalize the dataset in the range of 0–1, aiming to avoid overfitting the model. Therefore, a simple MLP neural network model with one hidden layer was selected for this aim. Different nodes varied from 4, 6, 8, 10, 12, 14, 16, 18, 20 to determine the optimum configuration of the MLP neural network. Finally, a simple MLP neural network with a hidden layer and 12 hidden nodes were defined to aim for Pb^{2+} absorption efficiency estimation (Fig. 8). It is worth mentioning that the back-propagation algorithm was applied during training the MLP

neural network model, and the ReLU activation function was used to process the data in the hidden layer.

Once the architecture of the MLP neural network was well-designed, the proposed flowchart in Fig. 7 was applied to develop the HHO-MLP neural network model. Accordingly, the HHO's parameters were set up first, as follow:

- (i) The number of populations: 10, 20, 30, 40, 50, 60, 70, 80, 90, 100
- (ii) Iterations: 1000
- (iii) Objective function :

$$MSE = \frac{1}{n_{Pb(II)}} \sum_{i=1}^{n_{Pb(II)}} (y_{Pb(II)} - \hat{y}_{Pb(II)})^2$$

Next, the HHO algorithm was performed to optimize the weights of the developed MLP neural network model through MSE values (Fig. 9). Finally, the optimal HHO-MLP neural network model was defined with an MSE of 1.873.

8 Results and discussion

As the innovations of this work, (1) nanotube-type halloysite in weathered pegmatites was used as the material to adsorb Pb^{2+} in an aqueous solution; and (2) the novel HHO-MLP neural network model was developed and proposed to estimate the Pb^{2+} absorption efficiency on nanotube-type halloysite in weathered pegmatites. Therefore, this section focused on evaluating the Pb^{2+} absorption efficiency of the

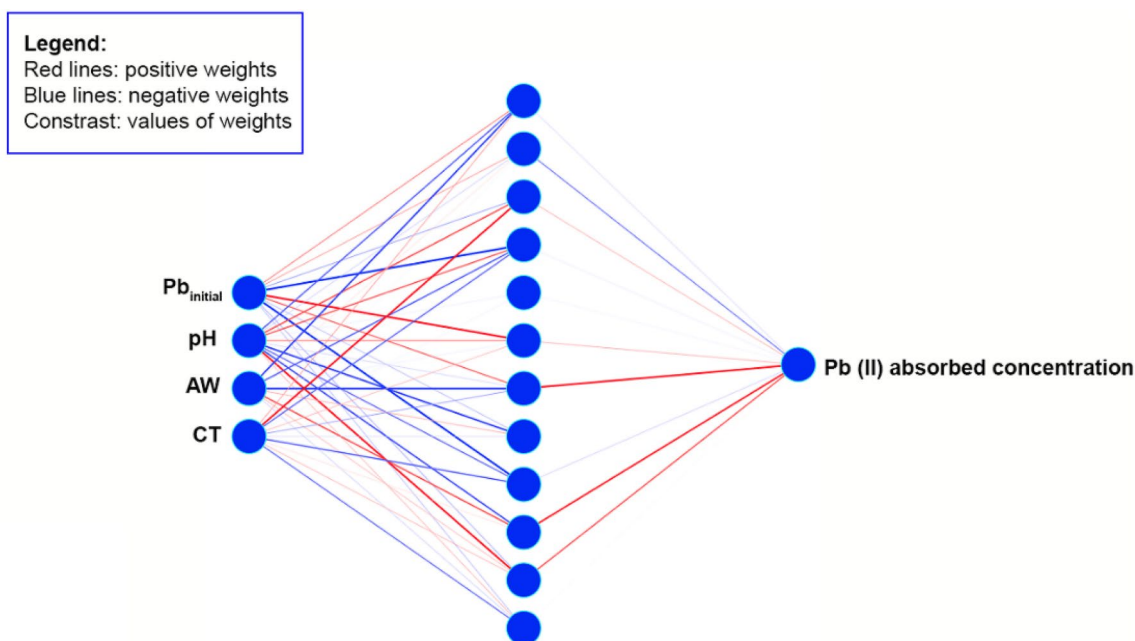


Fig. 8 The designed architecture of the MLP neural network for estimating the Pb^{2+} absorption efficiency in this study

Performance of the HHO-MLP neural network model

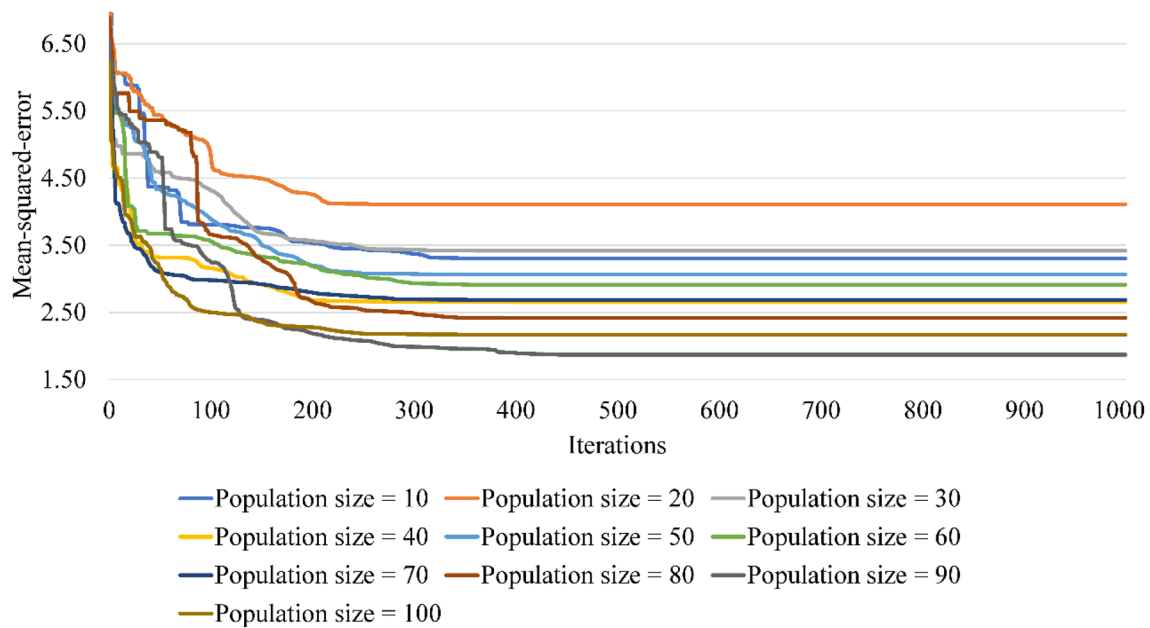


Fig. 9 The HHO-MLP neural network optimization model for predicting Pb^{2+} absorption efficiency

nanotube-type halloysite in weathered pegmatites and the proposed performance HHO-MLP neural network model.

Based on the experimental results, as shown in Fig. 3, it is unquestionable that the nanotube-type halloysite in weathered pegmatites is a robust material for the absorption of Pb^{2+} . The Pb^{2+} concentration was removed significantly after absorption by the nanotube-type halloysite in weathered pegmatites. Nevertheless, the absorption efficiency of different experiments is not the same, as shown in experiments No. 25 to No. 46. Although the initial Pb^{2+} concentration of these experiments is the same; however, the Pb^{2+} concentration after absorption is not the same. The main reason for these results is the different conditions of pH, adsorbent weight, and contact time. In other words, the absorption efficiency of Pb^{2+} is not similar with different input conditions. Therefore, a novel intelligent model with high accuracy of the absorption efficiency prediction is a good candidate and a perfect solution to adjust the input conditions to eliminate Pb^{2+} from water by the nanotube-type halloysite in weathered pegmatites.

Herein, the HHO-MLP neural network model was developed, and after the nanotube-type halloysite in weathered

pegmatites was well-evaluated in terms of the absorption of Pb^{2+} in water, the performance of the proposed HHO-MLP neural network in estimating Pb^{2+} absorption efficiency on nanotube-type halloysite in weathered pegmatites was taken into account through three performance metrics, such as MSE, RMSE, and R^2 . The proposed HHO-MLP neural network model was also compared with that of the MLP neural network model (without optimization) to demonstrate the proposed model's enhanced performance in estimating Pb^{2+} absorption efficiency nanotube-type halloysite in weathered pegmatites. Table 1 shows the MLP neural network's performance without and with the optimization of the HHO algorithm.

As shown in Table 1, the proposed HHO-MLP neural network provided an outstanding performance than those of the MLP neural network without optimizing by the HHO algorithm. Remarkable, the HHO-MLP's performances are excellent on both the training and testing dataset. Compared with that of the basic model (i.e., MLP neural network model without optimization), all three performance metrics of the proposed HHO-MLP neural network are better on the training and testing datasets. In other words, the accuracy of the

Table 1 Performance of the intelligent models for estimating the Pb^{2+} absorption efficiency on nanotube-type halloysite in weathered pegmatites

Predictive model	Performances on train			Performances on test		
	MSE	RMSE	R^2	MSE	RMSE	R^2
MLP	1.873	1.368	0.957	3.612	1.901	0.848
HHO-MLP	1.079	1.039	0.975	1.647	1.283	0.931

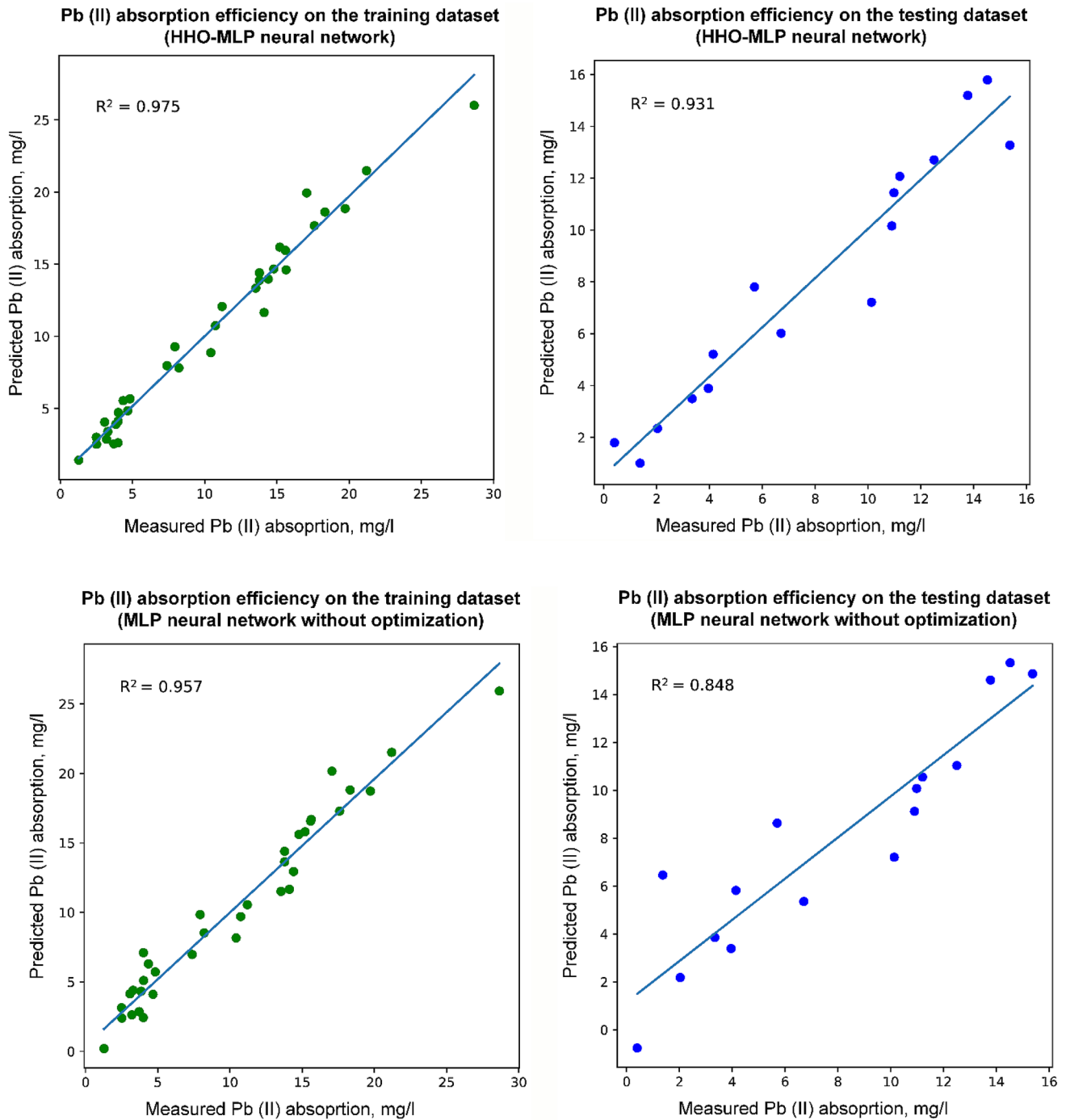


Fig. 10 Pb^{2+} absorption efficiency (measured versus predicted) on the proposed HHO-MLP neural network and MLP neural network (without optimization)

MLP neural network was significantly improved by the HHO algorithm, and it was increased from 9 to 10%. Figure 10 also indicated that the proposed HHO-MLP neural network model provided higher regression and convergence capabilities and better-explained relationships between variables. Notably, the proposed HHO-MLP neural network model's

regression and convergence capabilities on the testing dataset are superior (i.e., $R^2 = 0.931$) to those of the MLP neural network model without optimization (i.e., $R^2 = 0.848$).

To further assess the predictive models in estimating Pb^{2+} absorption efficiency on nanotube-type halloysite in weathered pegmatites, a Taylor diagram was established

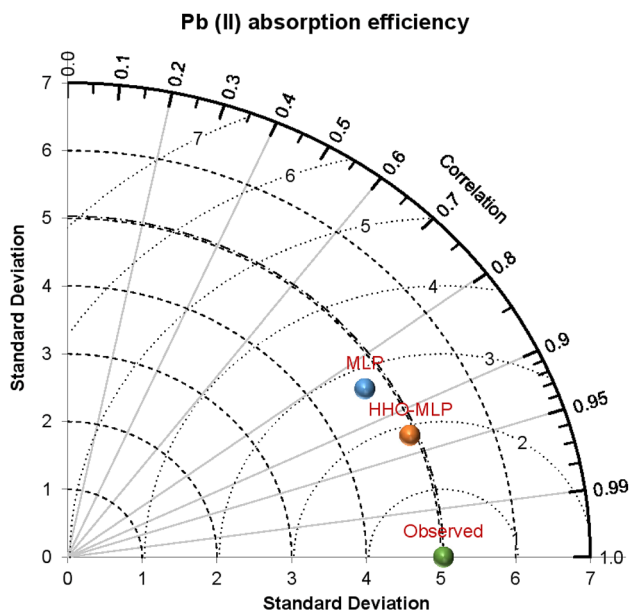


Fig. 11 Models' evaluation through the Taylor diagram

based on the actual values, standard deviation, correlation, and different MSE (Fig. 11). This diagram will explain how differences between the predictive models and the actual model. Indeed, we can see that the HHO-MLP neural network model's position on the diagram is closer to the actual model than those of the MLP neural network model. Also, the standard deviation of the proposed HHO-MLP neural network model is too dissimilar to the actual model's standard deviation value. These findings indicated that the proposed HHO-MLP neural network model is a reliable, intelligent model for estimating Pb^{2+} absorption efficiency on nanotube-type halloysite in weathered pegmatites, and the HHO algorithm significantly improved its reliability.

9 Validation of the models

To validate the proposed model in practice, 12 experiments were performed, and their parameters were also used as the inputs for the developed intelligent models. The predicted results were then compared with the experimental results to demonstrate the accuracy of the predictive models, as listed in Table 2.

Based on the experimental and predicted results in Table 2, the predicted values by the proposed HHO-MLP neural network model are very close to the experimental results. In contrast, the MLP neural network without optimization provided the predicted values with higher differences. Taking a look at Table 2 shows that all the 12 predicted values of the proposed HHO-MLP neural network model are better and more accurate than those of the predicted values given by the MLP neural network model. A regression graph in Fig. 12 interpreted the statistical relationship between actual and predicted individual models' values on the validation dataset. Accordingly, it explains how far the predicted values and actual values. The results in Fig. 12 showed that the predicted values by the MLP neural network are more different than the predicted values of the proposed HHO-MLP neural network model. Furthermore, evaluation on the three datasets: training, testing, and validation, the performance of the proposed HHO-MLP neural network model is highly stable, and the MLP neural network model provided a slightly lower stable between the training phase and testing, validating stages.

Table 2 Validation experiments and predicted values by the developed models

Initial concentration	pH	Volume	Reaction time	Conc. after absorption	Predicted by HHO-MLP	Predicted by MLP
80	5.13	0.8	50	18.278	16.617	21.613
80	5.39	0.7	25	20.534	18.739	25.954
50	5.50	0.5	55	6.757	9.181	8.493
45	5.46	0.7	40	4.252	6.029	7.792
30	5.06	0.5	80	9.992	9.473	8.800
40	4.31	0.6	95	7.062	8.525	7.424
80	6.13	0.6	100	6.702	8.992	3.442
40	4.83	0.3	35	20.029	19.305	17.526
35	5.15	0.6	45	5.961	7.459	6.933
60	6.00	0.4	80	7.69	8.929	9.551
35	6.02	0.3	95	7.327	6.752	12.216
55	5.08	0.5	95	6.106	7.840	8.556

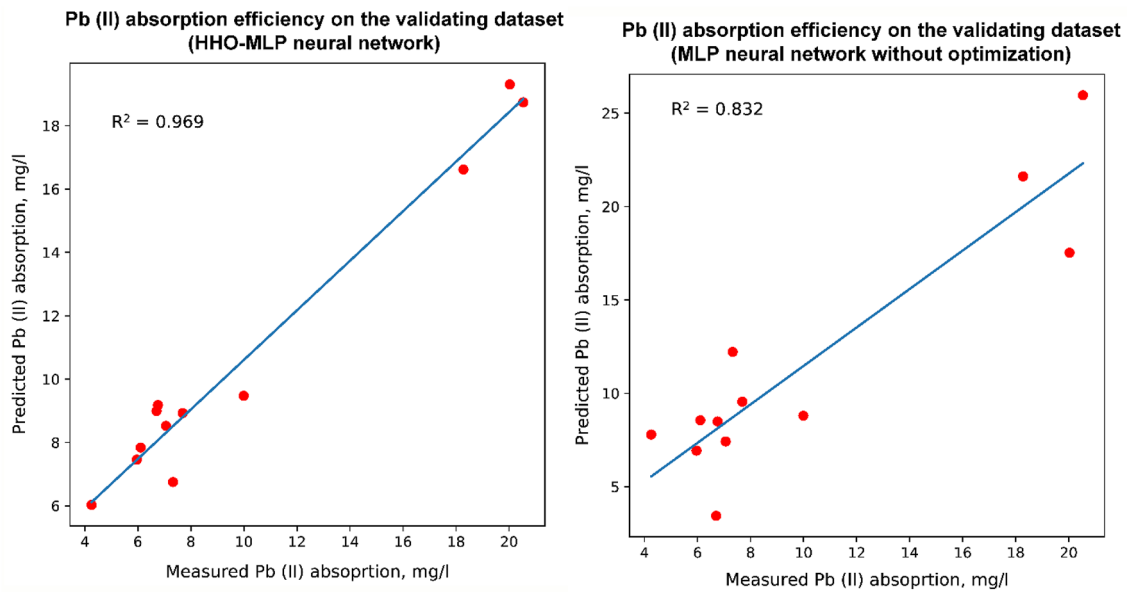


Fig. 12 Validation of the proposed HHO-MLP neural network and MLP neural network (without optimization) for estimating Pb^{2+} absorption efficiency

10 Conclusion and remarks

Nanotube-type halloysite in weathered pegmatites is a material applied to absorb Pb^{2+} in an aqueous solution with high efficiency. The experimental results showed that nanotube-type halloysite in weathered pegmatites could remove most Pb^{2+} in water. However, absorption performance is highly dependent on the pH, the volume of material, and reaction time. Therefore, this study developed and proposed a novel intelligent hybrid model, i.e., HHO-MLP neural network, for estimating Pb^{2+} absorption efficiency on nanotube-type halloysite in weathered pegmatites. The obtained results showed that the proposed HHO-MLP neural network model could estimate Pb^{2+} absorption efficiency in the water with high accuracy based on the influential parameters. Thereby, the influential parameters can be adjusted to remove Pb^{2+} from the aqueous solution completely using the proposed HHO-MLP neural network model.

The combination of nanotube-type halloysite in weathered pegmatites and the proposed HHO-MLP neural network to absorb Pb^{2+} in water can be taken into account as a robust and perfect system for water treatment plants. Whereas the nanotube-type halloysite in weathered pegmatites with robust Pb^{2+} absorption capacity, the proposed HHO-MLP neural network can accurately predict the concentration of Pb^{2+} after absorption by the nanotube-type halloysite in weathered pegmatites.

Although the obtained results were positive and the proposed HHO-MLP model can estimate Pb^{2+} absorption

efficiency in an aqueous solution using nanotube-type halloysite from weathered pegmatites with a promising result; however, there are many other heavy metals that need to be eliminated from an aqueous solution. Therefore, this study should be extended in the future to study the other heavy metals' absorption in an aqueous solution and the feasibility of nanotube-type halloysite from weathered pegmatites in the absorption of those heavy metals. In addition, a more extensive database is appropriate to understand further the characteristics of the absorbent used and heavy metals in an aqueous solution.

Acknowledgements This research was financially supported by the Vietnam National Foundation for Science and Technology Development (NAFOSTED), under Grant number 105.99-2017.317.

Declarations

Conflict of interest The authors declare that they do not have any conflicts in this paper.

References

1. Tran TTT, Pham HK, Nguyen HM (2020) Assessing the current status of rural domestic solid waste management in Nam Dinh province. *J Min Earth Sci* 61(6):82–89. [https://doi.org/10.46326/JMES.2020.61\(6\).09](https://doi.org/10.46326/JMES.2020.61(6).09)
2. Nguyen PHV, Phan TKT, Nguyen NT, Huynh TTT (2020) Effectiveness of *Moringa oleifera* seed powder as coagulant and reduction of TSS, COD, total coliform in the face water. *J Min*

- Earth Sci 61(1):101–109. [https://doi.org/10.46326/JMES.2020.61\(1\).11](https://doi.org/10.46326/JMES.2020.61(1).11)
3. Masindi V, Muedi KL (2018) Environmental contamination by heavy metals. *Heavy Met* 10:115–132
 4. Soltani N, Keshavarzi B, Moore F, Tavakol T, Lahijanzadeh AR, Jaafarzadeh N, Kermani M (2015) Ecological and human health hazards of heavy metals and polycyclic aromatic hydrocarbons (PAHs) in road dust of Isfahan metropolis, Iran. *Sci Total Environ* 505:712–723
 5. Carolin CF, Kumar PS, Saravanan A, Joshiba GJ, Naushad M (2017) Efficient techniques for the removal of toxic heavy metals from aquatic environment: a review. *J Environ Chem Eng* 5(3):2782–2799
 6. Kapoor D, Singh MP (2020) Heavy metal contamination in water and its possible sources. *Heavy metals in the environment*. Elsevier, pp 179–189
 7. Häder D-P, Banaszak AT, Villafañe VE, Narvarte MA, González RA, Helbling EW (2020) Anthropogenic pollution of aquatic ecosystems: emerging problems with global implications. *Sci Total Environ* 713:136586
 8. Islam A, Ahmad A, Laskar MA (2012) Characterization of a chelating resin functionalized via azo spacer and its analytical applicability for the determination of trace metal ions in real matrices. *J Appl Polym Sci* 123(6):3448–3458
 9. Nguyen NT (2020) Applying the Equivalent Plane Strain solution to design the soft soil improvement by vertical drains. *J Min Earth Sci* 61(3):28–37. [https://doi.org/10.46326/JMES.2020.61\(3\).04](https://doi.org/10.46326/JMES.2020.61(3).04)
 10. Petersen L, Heynen M, Pellicciotti F (2019) Freshwater resources: past, present, future. <https://doi.org/10.1002/9781118786352.wbieg0712.pub2>
 11. Kikkas KN, Kulik SV (2018) Modelling the effect of human activity on fresh water extraction from the earth's reserves. *IOP Conf. Ser.: Earth Environ. Sci.* 180:012017
 12. Peng W, Li H, Liu Y, Song S (2017) A review on heavy metal ions adsorption from water by graphene oxide and its composites. *J Mol Liq* 230:496–504. <https://doi.org/10.1016/j.molliq.2017.01.064>
 13. Liu X, Ma R, Wang X, Ma Y, Yang Y, Zhuang L, Zhang S, Jehan R, Chen J, Wang X (2019) Graphene oxide-based materials for efficient removal of heavy metal ions from aqueous solution: a review. *Environ Pollut* 252:62–73. <https://doi.org/10.1016/j.envpol.2019.05.050>
 14. Jiang H, Yang Y, Lin Z, Zhao B, Wang J, Xie J, Zhang A (2020) Preparation of a novel bio-adsorbent of sodium alginate grafted polyacrylamide/graphene oxide hydrogel for the adsorption of heavy metal ion. *Sci Total Environ* 744:140653. <https://doi.org/10.1016/j.scitotenv.2020.140653>
 15. Abubshait HA, Farag AA, El-Raouf MA, Negm NA, Mohamed EA (2020) Graphene oxide modified thiosemicarbazide nanocomposite as an effective eliminator for heavy metal ions. *J Mol Liq* 327:114790. <https://doi.org/10.1016/j.molliq.2020.114790>
 16. Zhu F, Zheng Y-M, Zhang B-G, Dai Y-R (2021) A critical review on the electrospun nanofibrous membranes for the adsorption of heavy metals in water treatment. *J Hazard Mater* 401:123608. <https://doi.org/10.1016/j.jhazmat.2020.123608>
 17. Choi HY, Bae JH, Hasegawa Y, An S, Kim IS, Lee H, Kim M (2020) Thiol-functionalized cellulose nanofiber membranes for the effective adsorption of heavy metal ions in water. *Carbohydr Polym* 234:115881. <https://doi.org/10.1016/j.carbpol.2020.115881>
 18. Abukhadra MR, Bakry BM, Adlii A, Yakout SM, El-Zaidy ME (2019) Facile conversion of kaolinite into clay nanotubes (KNTs) of enhanced adsorption properties for toxic heavy metals (Zn^{2+} , Cd^{2+} , Pb^{2+} , and Cr^{6+}) from water. *J Hazard Mater* 374:296–308. <https://doi.org/10.1016/j.jhazmat.2019.04.047>
 19. Ainscough TJ, Alagappan P, Oatley-Radcliffe DL, Barron AR (2017) A hybrid super hydrophilic ceramic membrane and carbon nanotube adsorption process for clean water production and heavy metal removal and recovery in remote locations. *J Water Process Eng* 19:220–230. <https://doi.org/10.1016/j.jwpe.2017.08.006>
 20. Liu C, Wang Q, Jia F, Song S (2019) Adsorption of heavy metals on molybdenum disulfide in water: a critical review. *J Mol Liq* 292:111390. <https://doi.org/10.1016/j.molliq.2019.111390>
 21. Ranjith KS, Manivel P, Rajendrakumar RT, Uyar T (2017) Multifunctional ZnO nanorod-reduced graphene oxide hybrids nanocomposites for effective water remediation: effective sunlight driven degradation of organic dyes and rapid heavy metal adsorption. *Chem Eng J* 325:588–600. <https://doi.org/10.1016/j.cej.2017.05.105>
 22. Tian Y, Wu M, Liu R, Li Y, Wang D, Tan J, Wu R, Huang Y (2011) Electrospun membrane of cellulose acetate for heavy metal ion adsorption in water treatment. *Carbohydr Polym* 83(2):743–748. <https://doi.org/10.1016/j.carbpol.2010.08.054>
 23. Vilardi G, Mpouras T, Dermatas D, Verdona N, Polydera A, Di Palma L (2018) Nanomaterials application for heavy metals recovery from polluted water: the combination of nano zero-valent iron and carbon nanotubes. *Comput Adsorpt Non-linear Model Chemosph* 201:716–729. <https://doi.org/10.1016/j.chemosphere.2018.03.032>
 24. Zheng X, Chen F, Zhang X, Zhang H, Li Y, Li J (2019) Ionic liquid grafted polyamide 6 as porous membrane materials: enhanced water flux and heavy metal adsorption. *Appl Surf Sci* 481:1435–1441. <https://doi.org/10.1016/j.apsusc.2019.03.111>
 25. Jahed Armaghani D, Harandizadeh H, Momeni E (2021) Load carrying capacity assessment of thin-walled foundations: an ANFIS–PNN model optimized by genetic algorithm. *Eng Comput* <https://doi.org/10.1007/s00366-021-01380-0>
 26. Armaghani DJ, Asteris PG (2021) A comparative study of ANN and ANFIS models for the prediction of cement-based mortar materials compressive strength. *Neural Comput Appl* 33(9):4501–4532. <https://doi.org/10.1007/s00521-020-05244-4>
 27. Armaghani DJ, Koopialipoor M, Marto A, Yagiz S (2019) Application of several optimization techniques for estimating TBM advance rate in granitic rocks. *J Rock Mech Geotech* 11(4):779–789. <https://doi.org/10.1016/j.jrmge.2019.01.002>
 28. Armaghani DJ, Koopialipoor M, Bahri Mahdi M, Hasanipanah M, Tahir M (2020) A SVR-GWO technique to minimize flyrock distance resulting from blasting. *Bull Eng Geol Environ* 79(8):4369–4385. <https://doi.org/10.1007/s10064-020-01834-7>
 29. Nguyen H (2020) Application of the k - nearest neighbors algorithm for predicting blast - induced ground vibration in open - pit coal mines: a case study. *J Min Earth Sci* 61(6):22–29. [https://doi.org/10.46326/JMES.2020.61\(6\).03](https://doi.org/10.46326/JMES.2020.61(6).03)
 30. Singh KP, Gupta S, Ojha P, Rai P (2013) Predicting adsorptive removal of chlorophenol from aqueous solution using artificial intelligence based modeling approaches. *Environ Sci Pollut Res* 20(4):2271–2287. <https://doi.org/10.1007/s11356-012-1102-y>
 31. Fawzy M, Nasr M, Nagy H, Helmi S (2018) Artificial intelligence and regression analysis for Cd(II) ion biosorption from aqueous solution by *Gossypium barbadense* waste. *Environ Sci Pollut Res* 25(6):5875–5888. <https://doi.org/10.1007/s11356-017-0922-1>
 32. Dolatabadi M, Mehrabpour M, Esfandyari M, Alidadi H, Davoudi M (2018) Modeling of simultaneous adsorption of dye and metal ion by sawdust from aqueous solution using of ANN and ANFIS. *Chemom Intell Lab Syst* 181:72–78. <https://doi.org/10.1016/j.chemolab.2018.07.012>
 33. Fan M, Hu J, Cao R, Ruan W, Wei X (2018) A review on experimental design for pollutants removal in water treatment with the aid of artificial intelligence. *Chemosphere* 200:330–343. <https://doi.org/10.1016/j.chemosphere.2018.02.111>

34. Lu H, Li H, Liu T, Fan Y, Yuan Y, Xie M, Qian X (2019) Simulating heavy metal concentrations in an aquatic environment using artificial intelligence models and physicochemical indexes. *Sci Total Environ* 694:133591. <https://doi.org/10.1016/j.scitotenv.2019.133591>
35. Rahnama E, Bazrafshan O, Asadollahfardi G (2020) Application of data-driven methods to predict the sodium adsorption rate (SAR) in different climates in Iran. *Arab J Geosci* 13(21):1160. <https://doi.org/10.1007/s12517-020-06146-4>
36. El Hanandeh A, Mahdi Z, Imtiaz MS (2021) Modelling of the adsorption of Pb, Cu and Ni ions from single and multi-component aqueous solutions by date seed derived biochar: comparison of six machine learning approaches. *Environ Res* 192:110338. <https://doi.org/10.1016/j.envres.2020.110338>
37. Rodríguez-Romero JA, Mendoza-Castillo DI, Reynel-Ávila HE, de Haro-Del Rio DA, González-Rodríguez LM, Bonilla-Petriciolet A, Duran-Valle CJ, Camacho-Aguilar KI (2020) Preparation of a new adsorbent for the removal of arsenic and its simulation with artificial neural network-based adsorption models. *J Environ Chem Eng* 8(4):103928. <https://doi.org/10.1016/j.jece.2020.103928>
38. Das A, Bar N, Das SK (2020) Pb(II) adsorption from aqueous solution by nutshells, green adsorbent: adsorption studies, regeneration studies, scale-up design, its effect on biological indicator and MLR modeling. *J Colloid Interface Sci* 580:245–255. <https://doi.org/10.1016/j.jcis.2020.07.017>
39. Fawzy M, Nasr M, Adel S, Nagy H, Helmi S (2016) Environmental approach and artificial intelligence for Ni(II) and Cd(II) biosorption from aqueous solution using *Typha domingensis* biomass. *Ecol Eng* 95:743–752. <https://doi.org/10.1016/j.ecoleng.2016.07.007>
40. Popoola LT (2019) Nano-magnetic walnut shell-rice husk for Cd(II) sorption: design and optimization using artificial intelligence and design expert. *Heliyon* 5(8):e02381. <https://doi.org/10.1016/j.heliyon.2019.e02381>
41. Qi J, Hou Y, Hu J, Ruan W, Xiang Y, Wei X (2020) Decontamination of methylene blue from simulated wastewater by the mesoporous rGO/Fe/Co nanohybrids: artificial intelligence modeling and optimization. *Mater Today Commun* 24:100709. <https://doi.org/10.1016/j.mtcomm.2019.100709>
42. Salehi E, Abdi J, Aliei MH (2016) Assessment of Cu(II) adsorption from water on modified membrane adsorbents using LS-SVM intelligent approach. *J Saudi Chem Soc* 20(2):213–219. <https://doi.org/10.1016/j.jscs.2014.02.007>
43. Shojaeimehr T, Rahimpour F, Khadivi MA, Sadeghi M (2014) A modeling study by response surface methodology (RSM) and artificial neural network (ANN) on Cu²⁺ adsorption optimization using light expanded clay aggregate (LECA). *J Ind Eng Chem* 20(3):870–880. <https://doi.org/10.1016/j.jiec.2013.06.017>
44. Souza PR, Dotto GL, Salau NPG (2018) Artificial neural network (ANN) and adaptive neuro-fuzzy interference system (ANFIS) modelling for nickel adsorption onto agro-wastes and commercial activated carbon. *J Environ Chem Eng* 6(6):7152–7160. <https://doi.org/10.1016/j.jece.2018.11.013>
45. Zafar M, Van Vinh N, Behera SK, Park H-S (2017) Ethanol mediated As(III) adsorption onto Zn-loaded pinecone biochar: experimental investigation, modeling, and optimization using hybrid artificial neural network-genetic algorithm approach. *J Environ Sci* 54:114–125. <https://doi.org/10.1016/j.jes.2016.06.008>
46. Zhao L, Dai T, Qiao Z, Sun P, Hao J, Yang Y (2020) Application of artificial intelligence to wastewater treatment: a bibliometric analysis and systematic review of technology, economy, management, and wastewater reuse. *Process Saf Environ Prot* 133:169–182. <https://doi.org/10.1016/j.psep.2019.11.014>
47. Gu Z, Song W, Yang Z, Zhou R (2018) Metal–organic framework as an efficient filter for the removal of heavy metal cations in water. *Phys Chem Chem Phys* 20(48):30384–30391
48. Ghorbani YA, Ghoreishi SM, Ghani M (2020) Derived N-doped carbon through core-shell structured metal-organic frameworks as a novel sorbent for dispersive solid phase extraction of Cr(III) and Pb(II) from water samples followed by determination through flame atomic absorption spectrometry. *Microchem J* 155:104786
49. Bui H-B, Nguyen T-D (2016) Finding of halloysite nanotubes in Lang Dong kaolin deposit, Phu Tho province. *Vietnam J Earth Sci* 34(3):275–280
50. Bac BH, Dung NT, Khang LQ, Lam NV, An DM, Son PV, Anh TTV, Chuong DV, Tinh BT (2018) Distribution and characteristics of nanotubular halloysites in the Thach Khoan Area, Phu Tho, Vietnam. *Minerals* 8(7):290
51. Nguyen H, Bui X-N (2018) Predicting blast-induced air overpressure: a robust artificial intelligence system based on artificial neural networks and random forest. *Nat Resour Res* 28(3):893–907
52. Guo H, Nguyen H, Vu D-A, Bui X-N (2019) Forecasting mining capital cost for open-pit mining projects based on artificial neural network approach. *Resour Policy*. <https://doi.org/10.1016/j.resourpol.2019.101474>
53. Nguyen H, Bui H-B, Bui X-N (2020) Rapid determination of gross calorific value of coal using artificial neural network and particle swarm optimization. *Nat Resour Res*. <https://doi.org/10.1007/s11053-020-09727-y>
54. Zhang H, Nguyen H, Bui X-N, Nguyen-Thoi T, Bui T-T, Nguyen N, Vu D-A, Mahesh V, Moayedi H (2020) Developing a novel artificial intelligence model to estimate the capital cost of mining projects using deep neural network-based ant colony optimization algorithm. *Resour Policy* 66:101604
55. Nguyen H, Bui X-N, Bui H-B, Mai N-L (2018) A comparative study of artificial neural networks in predicting blast-induced air-blast overpressure at Deo Nai open-pit coal mine, Vietnam. *Neural Comput Appl* 32(8):3939–3955. <https://doi.org/10.1007/s00521-018-3717-5>
56. Nguyen H, Drebenstedt C, Bui X-N, Bui DT (2019) Prediction of blast-induced ground vibration in an open-pit mine by a novel hybrid model based on clustering and artificial neural network. *Nat Resour Res* 29(2):691–709
57. Lin T-L, Tseng H-W, Wen Y, Lai F-W, Lin C-H, Wang C-J (2018) Reconstruction algorithm for lost frame of multiview videos in wireless multimedia sensor network based on deep learning multilayer perceptron regression. *IEEE Sens J* 18(23):9792–9801
58. Luo C, Wu D, Wu D (2017) A deep learning approach for credit scoring using credit default swaps. *Eng Appl Artif Intell* 65:465–470
59. Golovko V (2017) Deep learning: an overview and main paradigms. *Opt Mem Neural Netw* 26(1):1–17
60. Guo Y, Liu Y, Oerlemans A, Lao S, Wu S, Lew MS (2016) Deep learning for visual understanding: a review. *Neurocomputing* 187:27–48
61. Fawaz HI, Forestier G, Weber J, Idoumghar L, Muller P-A (2019) Deep learning for time series classification: a review. *Data Min Knowl Discov* 33(4):917–963
62. Shrestha A, Mahmood A (2019) Review of deep learning algorithms and architectures. *IEEE Access* 7:53040–53065
63. Heidari AA, Mirjalili S, Faris H, Aljarah I, Mafarja M, Chen H (2019) Harris hawks optimization: algorithm and applications. *Future Gener Comput Syst* 97:849–872
64. Al-Betar MA, Awadallah MA, Heidari AA, Chen H, Al-khraisat H, Li C (2020) Survival exploration strategies for Harris hawks optimizer. *Expert Syst Appl* 168:114243. <https://doi.org/10.1016/j.eswa.2020.114243>

65. Qu C, He W, Peng X, Peng X (2020) Harris hawks optimization with information exchange. *Appl Math Model* 84:52–75. <https://doi.org/10.1016/j.apm.2020.03.024>
66. Song S, Wang P, Heidari AA, Wang M, Zhao X, Chen H, He W, Xu S (2020) Dimension decided Harris hawks optimization with Gaussian mutation: balance analysis and diversity patterns. *Knowl-Based Syst* 215:106425. <https://doi.org/10.1016/j.knosys.2020.106425>
67. Beşkirli A, Dağ İ (2020) A new binary variant with transfer functions of Harris hawks optimization for binary wind turbine micro-siting. *Energy Rep* 6:668–673. <https://doi.org/10.1016/j.egy.2020.11.154>
68. Gölcük İ, Özsoydan FB (2020) Quantum particles-enhanced multiple Harris hawks swarms for dynamic optimization problems. *Expert Syst Appl* 167:114202. <https://doi.org/10.1016/j.eswa.2020.114202>
69. Jiao S, Chong G, Huang C, Hu H, Wang M, Heidari AA, Chen H, Zhao X (2020) Orthogonally adapted Harris hawks optimization for parameter estimation of photovoltaic models. *Energy* 203:117804. <https://doi.org/10.1016/j.energy.2020.117804>
70. Liu Y, Chong G, Heidari AA, Chen H, Liang G, Ye X, Cai Z, Wang M (2020) Horizontal and vertical crossover of Harris hawk optimizer with Nelder–Mead simplex for parameter estimation of photovoltaic models. *Energy Convers Manag* 223:113211. <https://doi.org/10.1016/j.enconman.2020.113211>
71. Shao K, Fu W, Tan J, Wang K (2020) Coordinated approach fusing time-shift multiscale dispersion entropy and vibrational Harris hawks optimization-based SVM for fault diagnosis of rolling bearing. *Measurement* 173:108580. <https://doi.org/10.1016/j.measurement.2020.108580>
72. Singh P, Prakash S (2020) Optimizing multiple ONUs placement in Fiber-Wireless (FiWi) access network using grasshopper and Harris hawks optimization algorithms. *Opt Fiber Technol* 60:102357. <https://doi.org/10.1016/j.yofte.2020.102357>
73. Yousri D, Allam D, Eteiba MB (2020) Optimal photovoltaic array reconfiguration for alleviating the partial shading influence based on a modified harris hawks optimizer. *Energy Convers Manag* 206:112470. <https://doi.org/10.1016/j.enconman.2020.112470>
74. Moayed H, Mu'azu Mohammed Abdullahi, Nguyen H, Rashid ASA (2021) Comparison of dragonfly algorithm and Harris hawks optimization evolutionary data mining techniques for the assessment of bearing capacity of footings over two-layer foundation soils. *Eng Comput* 37:437–447. <https://doi.org/10.1007/s00366-019-00834-w>

Publisher's Note Springer Nature remains neutral with regard to jurisdictional claims in published maps and institutional affiliations.